added (16), and phospho–MBP-Sic1p$^{myc\text{-}his6}$ was purified away from the reaction components by adsorption to 9E10 beads (monoclonal antibody to myc covalently coupled to protein A–Sepharose). Beads were washed twice with 25 mM tris (pH 8.0), 500 mM NaCl, and 0.2% octylglucoside, then twice with 25 mM tris (pH 6.8). Phospho–MBP-Sic1p$^{myc\text{-}his6}$ was eluted with 0.1% TFA, and the eluted protein was lyophilized in a Speedvac and reconstituted in 50 mM tris (pH 8.8) and 2 M urea.

29. MBP-Sic1$^{myc\text{-}his6}$ was isolated from BL21(DE3) cells containing pLysS by means of consecutive fractionations on Ni-NTA (Qiagen) and amylose (New England BioLabs) affinity resins according to the manufacturer's recommended procedures. In Fig. 4, [^{35}S]-labeled MBP-Sic1p$^{myc\text{-}his6}$ was expressed and purified from Tran^{35}S-labeled *E. coli* cells as described (26).
30. ^{32}P-labeled cells were harvested, vortexed with glass beads (0.5 mm), and then boiled in 2× lysis buffer containing 100 mM tris (pH 7.5), 2% SDS, 200 mM NaCl, 30 mM DTT, and a protease and phosphatase inhibitor cocktail (16). Cell lysates were diluted to a final concentration of 0.2% SDS with an immunoprecipitation buffer containing 50 mM tris (pH 7.5), 500 mM NaCl, 1% Triton X-100, and the phosphatase and protease inhibitor cocktails described above. Diluted lysates were centifuged at 15,000*g* for 15 min and supplemented with antiserum to Sic1p and protein A beads. Beads were washed three times with immunoprecipitation buffer and twice with 50 mM tris (pH 7.5) and were resuspended in 2× SDS sample buffer.
31. All singly and multiply mutated forms of *SIC1* were generated by a polymerase chain reaction (PCR)–based strategy (26) . PCR was done with 5' oligos containing T7 promoter sequences, and with a 3' oligo incorporating an HA epitope tag. Details are available upon request. In vitro transcription and translation of wild-type and mutant PCR templates were done as described (26).
32. The percentage of high-molecular-weight (HMW) ubiquitin conjugates formed was calculated by dividing the signal corresponding to ubiquitinated Sic1p^{HA} formed during a 30-min incubation in vitro by the total amount of Sic1^{HA} translation product present at the start of the reaction. Wild-type Sic1p^{HA} (65% of which was converted to HMW ubiquitin conjugates) was arbitrarily assigned a relative value of 1.0.
33. C. B. Epstein and F. R. Cross, *Genes Dev.* **6**, 1695 (1992).
34. We thank M. V. Castillo for MBP-SIC1, L. Johnston for Sic1p antiserum, S. Diamond for performing flow cytometry, J. Archer, B. Dunphy, and W. Shou for critically reading the manuscript, and members of the laboratory for helpful discussions. Supported in part by Searle/Chicago Community Trust and Lucille P. Markey Charitable Trust Scholar Awards to R.J.D. and by a grant from NIH (NIH RO1 GM52466-01).

16 June 1997; accepted 18 September 1997

CDC20 and *CDH1*: A Family of Substrate-Specific Activators of APC-Dependent Proteolysis

Rosella Visintin, Susanne Prinz, Angelika Amon*

Proteolysis mediated by the anaphase-promoting complex (APC) triggers chromosome segregation and exit from mitosis, yet its regulation is poorly understood. The conserved Cdc20 and Cdh1 proteins were identified as limiting, substrate-specific activators of APC-dependent proteolysis. *CDC20* was required for the degradation of the APC substrate Pds1 but not for that of other APC substrates, such as Clb2 and Ase1. Conversely, *cdh1*Δ mutants were impaired in the degradation of Ase1 and Clb2 but not in that of Pds1. Overexpression of either *CDC20* or *CDH1* was sufficient to induce APC-dependent proteolysis of the appropriate target in stages of the cell cycle in which substrates are normally stable.

Progression through mitosis requires the precisely timed ubiquitin-dependent degradation of specific substrates. In budding yeast, degradation of the Pds1 protein is required for the transition from metaphase to anaphase in the cell cycle (*1*). Exit from mitosis is initiated by proteolysis of mitotic cyclins (*2*). Destruction of the mitotic spindle–associated protein Ase1 is important for the disassembly of the mitotic spindle during exit from mitosis (*3*). Degradation of all these proteins is mediated by a 20S particle called the cyclosome or APC, which functions as a ubiquitin-protein ligase (*4*, *5*). The stability of substrates of the APC-dependent proteolysis machinery varies greatly during the cell cycle. Substrates are stable during S phase, G_2 phase, and early mitosis (M) phase but are highly unstable during exit from M phase and G_1 phase (*1*, *3*, *6*–*8*). Work in embryonic extracts has shown that APC activity is cell cycle regulated, suggesting that the activity of the APC determines whether APC substrates are degraded or not (*4*, *5*). However, degradation of different APC substrates is not coordinated, because temporal differences are observed (*9*–*11*). The proteolysis of APC substrates, therefore, cannot simply be regulated by the activation or inactivation of APC. Regulation must also occur at the level of specific substrates. We identified two highly conserved *Saccharomyces cerevisiae* proteins that function in this manner. Cdc20 and Cdh1 are substrate-specific activators of APC-dependent proteolysis.

To identify regulators of APC-dependent proteolysis, we screened previously identified temperature-sensitive cell division cycle (*cdc*) mutants for defects in APC-dependent proteolysis. Among these, mutants defective in the *CDC20* gene, which encodes a protein containing seven WD40 repeats (*12*), were of particular interest. *Saccharomyces cerevisiae cdc20-1* mutants and *Drosophila* mutants defective in the *fizzy* gene, a *CDC20* homolog, arrest in metaphase before the activation of the APC-dependent proteolytic program (*11*–*14*). To analyze the effects of the *cdc20-1* mutation on APC-dependent proteolysis, we took advantage of the fact that in yeast all known APC substrates (the mitotic cyclins Clb2 and Clb3, Pds1, and Ase1) are unstable during G_1 phase because of continuous APC-dependent proteolysis (*1*, *3*, *7*, *15*). Wild-type and *cdc20-1* cells were arrested at the permissive temperature in G_1 phase by exposure to the mating pheromone α-factor, and the half-lives of Clb2, Pds1, and Ase1 were determined after transient expression of their respective genes from the galactose (Gal)-inducible *GAL1-10* promoter and inactivation of *CDC20* by temperature shift (*16*). The *cdc20-1* mutation had little if any effect on the half-life of Clb2 (Fig. 1, A and B), which is consistent with the finding that the *cdc20-1* mutation does not affect ubiquitination of Clb2 in G_1 phase extracts (*15*). Similarly, the *cdc20-1* mutation had little if any effect on the half-life of Ase1 during G_1 phase (Fig. 1, C and D). In contrast, the half-life of Pds1 was prolonged in the *cdc20-1* mutant; Pds1 protein declined rapidly in wild-type cells but not in *cdc20-1* mutants (Fig. 1, E and F). These results indicate that *cdc20-1* mutants are defective in the degradation of Pds1 but not in that of Clb2 and Ase1 during the G_1 phase.

Because *CDC20* was required for the degradation of Pds1, we hypothesized that overexpression of *CDC20* might hasten the degradation of Pds1. To test this hypothesis, we treated exponentially growing cells carrying *CDC20* under the control of the *GAL1-10* promoter (*17*) with Gal to induce increased expression of *CDC20*. Although overexpression of *CDC20* did not affect the amount of *PDS1* RNA (*18*), the bulk of Pds1 protein disappeared within 60 min of Gal addition (Fig. 2A). In contrast, overexpression of *CDC20* had little if any effect on the total amounts of Clb2 or Ase1 protein (Fig. 2A). The decline in the amount of Pds1 brought about by overexpression of *CDC20* was prohibited in cells carrying a

Whitehead Institute for Biomedical Research, Nine Cambridge Center, Cambridge, MA 02142, USA.

*To whom correspondence should be addressed.

temperature-sensitive allele of *CDC23* (*cdc23-1*, which encodes a component of the APC), suggesting that the decline was dependent on APC-dependent proteolysis. Similar results were obtained with cells arrested in S phase by hydroxyurea, in which Clb2 and Pds1 are stable (*1*, *7*). Overexpression of *CDC20* led to a decrease in the amount of Pds1 in a *CDC23*-dependent manner, although somewhat less efficiently than in exponentially growing cells (Fig. 2B). In contrast, overexpression of *CDC20* did not affect the total amounts of Clb2 or Ase1 protein (Fig. 2B). In cells treated with the microtubule-depolymerizing drug nocodazole, Clb2, Pds1, and Ase1 are stable (*1*, *3*, *7*). Overexpression of *CDC20* in this arrest induced a decline in the amount of Pds1, Clb2, and, to a lesser degree, Ase1 (Fig. 2C). Whereas Clb2 normally has a half-life of more than 120 min in nocodazole-arrested cells (*7*), the bulk of Pds1 and Clb2 protein decayed within 30 min, suggesting that rapid protein degradation was responsible for the decreased amounts of Pds1 and Clb2. Indeed, degradation was delayed (in the case of Pds1) or prevented (for Clb2 and Ase1) in cells carrying a *cdc23-1* mutation (Fig. 2C). These results indicate that overexpression of *CDC20* is sufficient to induce APC-dependent degradation of Pds1 in stages of the cell cycle when Pds1 is normally stable but that it does not affect Clb2 and Ase1 protein. However, this specificity is partially lost in cells arrested with nocodazole.

Our findings raised the question whether factors exist that regulate the degradation of Clb2 and Ase1. A FASTA search (*19*) against all translated open reading frames (ORFs) of the *S. cerevisiae* genome identified the ORF YGL003C as similar to that of *CDC20* (*20*). We termed this ORF *CDH1* for *CDC20* homolog 1. Computer searches of protein sequence databases with BLASTP (*21*) revealed that *CDC20* and *CDH1* are highly conserved among all eukaryotes and that *Schizosaccharomyces pombe* and *Caenorhabditis elegans* also contain at least two members of the *CDC20*/*CDH1* family.

Deletion of *CDH1* (*22*) had little effect on viability and cell cycle progression. Cells grew more slowly, and there was a slight increase in cells with long anaphase spindles in exponentially growing cultures (20% compared with 14% in wild-type cells). We also analyzed the consequences of deleting *CDH1* for the stability of Pds1, Clb2, and Ase1. Wild-type G_1 phase cells obtained by

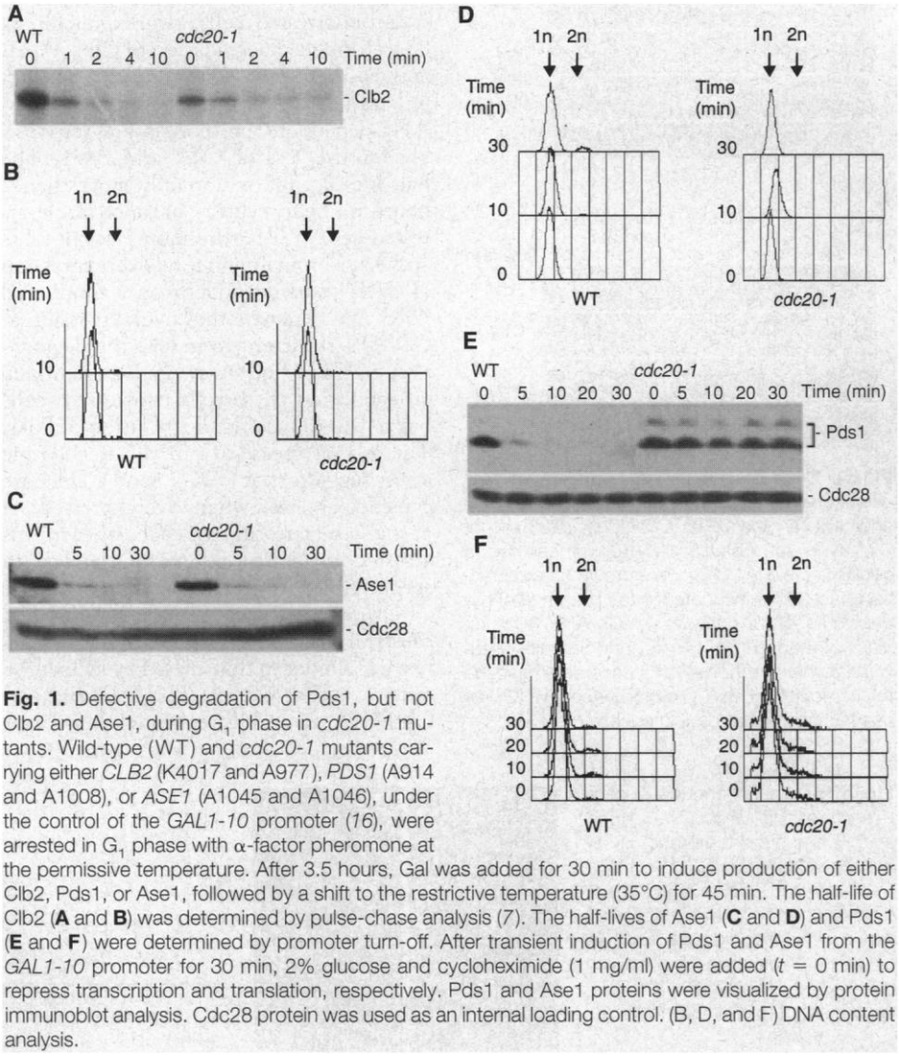

Fig. 1. Defective degradation of Pds1, but not Clb2 and Ase1, during G_1 phase in *cdc20-1* mutants. Wild-type (WT) and *cdc20-1* mutants carrying either *CLB2* (K4017 and A977), *PDS1* (A914 and A1008), or *ASE1* (A1045 and A1046), under the control of the *GAL1-10* promoter (*16*), were arrested in G_1 phase with α-factor pheromone at the permissive temperature. After 3.5 hours, Gal was added for 30 min to induce production of either Clb2, Pds1, or Ase1, followed by a shift to the restrictive temperature (35°C) for 45 min. The half-life of Clb2 (**A** and **B**) was determined by pulse-chase analysis (*7*). The half-lives of Ase1 (**C** and **D**) and Pds1 (**E** and **F**) were determined by promoter turn-off. After transient induction of Pds1 and Ase1 from the *GAL1-10* promoter for 30 min, 2% glucose and cycloheximide (1 mg/ml) were added (t = 0 min) to repress transcription and translation, respectively. Pds1 and Ase1 proteins were visualized by protein immunoblot analysis. Cdc28 protein was used as an internal loading control. (B, D, and F) DNA content analysis.

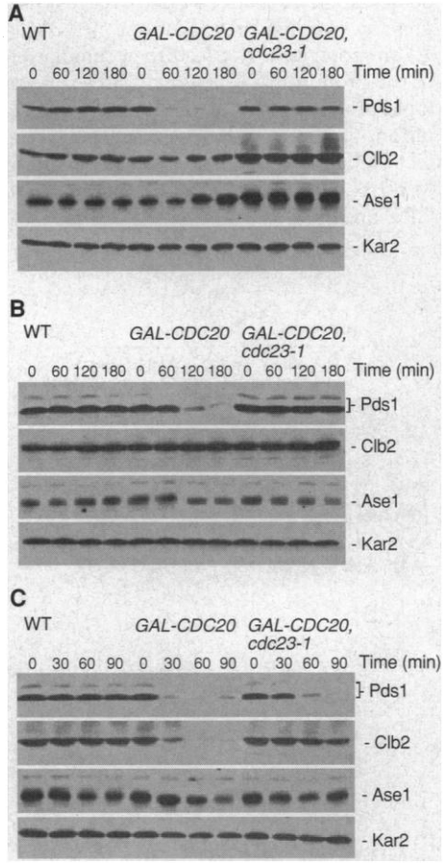

Fig. 2. Degradation of Pds1 induced by overexpression of *CDC20*. Wild-type cells (A1015) and cells carrying a *GAL-CDC20* fusion (*17*), either wild type for *CDC23* (A1016) or carrying a *cdc23-1* allele (A1022), were grown to exponential phase (**A**) or incubated in the presence of hydroxyurea (10 mg/ml) (**B**) or nocodazole (15 μg/ml) (**C**). After 3 hours, Gal was added (t = 0 min), and samples were withdrawn at the indicated times to determine total amounts of Pds1, Clb2, and Ase1 protein by protein immunoblot analysis. Kar2 protein was used as an internal loading control. The experiments were carried out at 23°C because expression of *CDC20* from the *GAL1-10* promoter was weak at 37°C. However, *cdc23-1* mutants are partly defective in Clb2 degradation even at 23°C (*29*). Because the experiment was carried out at 23°C, *cdc23-1* mutants presumably retained some activity that could account for the incomplete inhibition of Pds1 degradation in the nocodazole arrest.

centrifugal elutriation (*23*) lacked Clb2, Pds1, and Ase1 protein because of the lack of transcription and continuous proteolysis (Fig. 3A) (*1*, *3*, *7*). In contrast, elutriated *cdh1*Δ cells lacked Pds1 but contained abnormally large amounts of Clb2 and Ase1 (Fig. 3A). In *cdh1*Δ cells, similar amounts of Clb2 and Ase1 were present in G_1, S (hydroxyurea arrest), and M phases (nocodazole arrest), suggesting that their abundance does not fluctuate substantially during the cell cycle. This may be a consequence of defects in protein degradation rather than deregulation of transcription. Even overexpression of *CLB2* or *ASE1* from the *GAL1-10* promoter does not lead to accumulation of the protein in G_1 phase cells, because of rapid proteolysis (*3*, *7*). Thus, one interpretation of this result is that cells lacking *CDH1* had degraded Pds1 during exit from M phase but that they had failed to degrade Clb2 and Ase1.

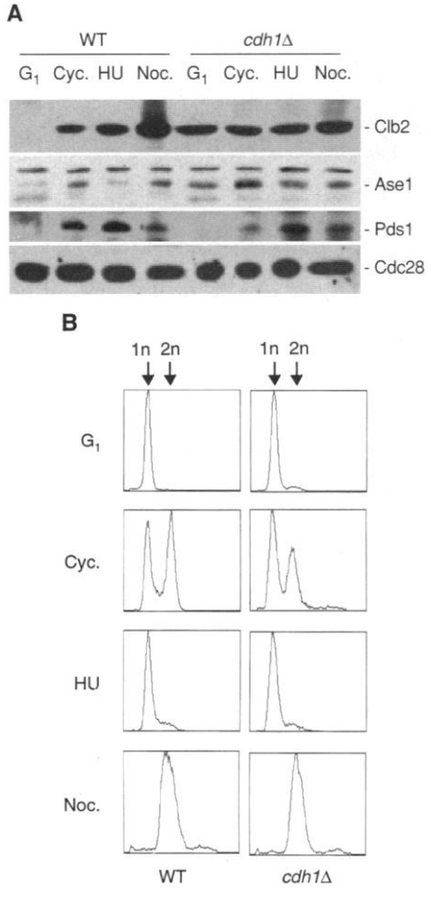

Fig. 3. Presence of Clb2 and Ase1 during G_1 phase in *cdh1*Δ mutants. Wild-type cells (A1015) or *cdh1::HIS3* (*cdh1*Δ) mutants (A1120) were elutriated to obtain small G_1 phase cells or arrested with nocodazole (Noc.) or hydroxyurea (HU) (*23*). (**A**) Clb2, Pds1, and Ase1. Cdc28 was used as an internal loading control. Cyc., cycling. (**B**) DNA content analysis.

Although the amount of Clb2 did not fluctuate much during the cell cycle in *cdh1*Δ cells, *cdh1*Δ mutants were viable, suggesting that degradation of mitotic cyclins might not be absolutely required for exit from M phase. This observation is consistent with previous findings. Moderate amounts of nondestructible Clb2 do not affect exit from M phase (*7*). Under conditions at which proteolysis of mitotic cyclins is impaired, mitotic kinase inhibition by the kinase inhibitor Sic1 (*24*) might be sufficient to trigger exit from M phase. Thus, inactivation of both Sic1 and proteolysis of mitotic cyclins (by deletion of *CDH1*) should be lethal. Indeed, we found such cells to be inviable. *cdh1*Δ, *sic1*Δ double-mutant spores germinated but arrested as large budded cells after one to three divisions.

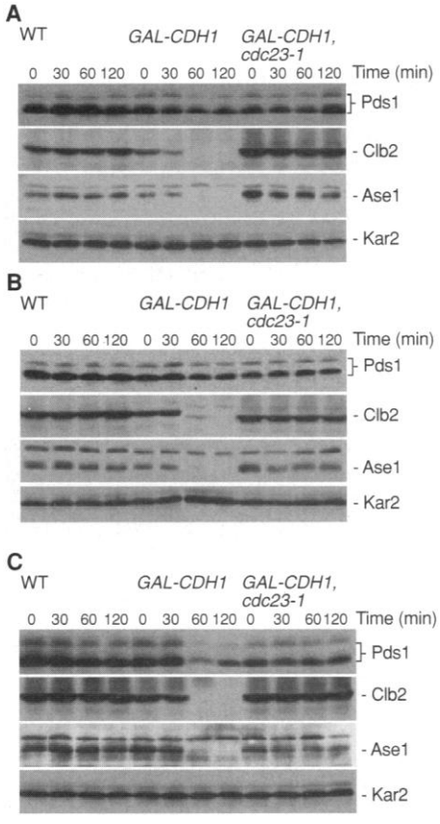

Fig. 4. Degradation of Clb2 and Ase1 in cells overexpressing *CDH1*. Wild-type cells (A1015) and cells carrying a *GAL-CDH1* fusion (*22*), either wild type for *CDC23* (A1110) or carrying a *cdc23-1* allele (A1112), were grown to exponential phase (**A**) or incubated in the presence of hydroxyurea (**B**) or nocodazole (**C**). After 3 hours, Gal was added (t = 0 min), and samples were withdrawn at the indicated times to determine the total amount of Pds1, Clb2, and Ase1. Kar2 was used as an internal loading control.

If *CDH1* is important for Clb2 and Ase1 degradation, overexpression of *CDH1* might induce ectopic degradation of Clb2 and Ase1. Exponentially growing cells carrying a *GAL-CDH1* fusion (*22*) were treated with Gal to induce the expression of *CDH1*. Within 60 min of Gal addition, the bulk of Clb2 and Ase1 disappeared (Fig. 4A). This decline was absent in a *cdc23-1* mutant, suggesting that it was a result of APC-dependent proteolysis. In contrast, overexpression of *CDH1* had only minor effects on the total amount of Pds1 (Fig. 4A). Similar results were obtained with cells arrested in S phase with hydroxyurea (Fig. 4B). In nocodazole-arrested cells, overexpression of *CDH1* induced degradation of Clb2, Ase1, and, to some extent, Pds1 (Fig. 4C). It is unlikely that mechanisms other than APC-dependent proteolysis are responsible for the loss of Clb2 and Ase1. The half-life of Clb2 is normally more than 2 hours in hydroxyurea- or nocodazole-arrested cells (*7*). Furthermore, loss of Clb2 and Ase1 brought about by overexpression of *CDH1* was dependent on a functional APC. We conclude that overexpression of *CDH1* is sufficient to induce the degradation of Clb2 and Ase1 in exponentially growing and hydroxyurea-arrested cells but not to induce the degradation of Pds1. The loss of specificity in the nocodazole arrest suggests that *CDC20* and *CDH1* are capable, at least when overexpressed, of partially substituting for each other in this arrest point. The reasons for the loss in specificity are at present unclear.

Overexpression of *CDH1* was lethal and caused a specific cell cycle arrest. This arrest was similar to that caused by lack of the mitotic cyclins *CLB1*, *CLB2*, *CLB3*, and *CLB4* (*25*, *26*). Cells replicated their DNA

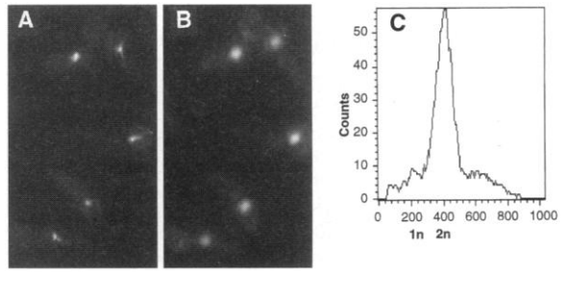

Fig. 5. Terminal phenotype of cells overexpressing *CDH1*. The mitotic spindle and nuclear morphology of cells overexpressing *CDH1* (A1110) were analyzed 2 hours after Gal addition by indirect immunofluorescence with antibodies to tubulin (**A**) or by 4′,6′-diamidino-2-phenylindole (DAPI) staining (**B**). (**C**) DNA content 4 hours after Gal addition.

but arrested with an elongated bud, lacking a bipolar mitotic spindle (Fig. 5). This phenotype is consistent with our findings that overexpression of *CDH1* induces degradation of mitotic cyclins.

We have identified a family of highly conserved WD40-repeat proteins as limiting activators of APC-dependent proteolysis. Cdc20 and Cdh1 were not general activators of APC-dependent proteolysis, but instead they appeared to be substrate specific. The WD40-repeat protein Cdc4 also serves as a specificity factor in the degradation of substrates of the Skp1/Cdc53-dependent proteolysis machinery (*27*). Specificity factors may facilitate the differential regulation of various substrates ubiquitinated by the same ubiquitination machinery. Cdc20 and Cdh1 may ensure that different substrates of the APC are degraded at the right time during M phase. Cdc20 may target APC substrates whose degradation is required for the metaphase-anaphase transition (such as Pds1) for degradation, whereas Cdh1 may trigger destruction of substrates whose degradation is important for exit from M phase (such as Clb2 and Ase1). Cdc20 homologs in other species may also be substrate-specific activators of APC-dependent proteolysis.

REFERENCES AND NOTES

1. O. Cohen-Fix, J.-M. Peters, M. W. Kirschner, D. Koshland, *Genes Dev.* **10**, 3081 (1996).
2. R. W. King, R. J. Deshaies, J.-M. Peters, M. W. Kirschner, *Science* **274**, 1652 (1996).
3. Y.-L. Juang *et al.*, *ibid.* **275**, 1311 (1997).
4. R. W. King *et al.*, *Cell* **81**, 279 (1995).
5. V. Sudakin *et al.*, *Mol. Biol. Cell* **6**, 185 (1995).
6. T. Evans, E. T. Rosenthal, J. Youngblom, D. Distel, T. Hunt, *Cell* **33**, 389 (1983).
7. A. Amon, S. Irniger, K. Nasmyth, *ibid.* **77**, 1037 (1994).
8. M. Brandeis and T. Hunt, *EMBO J.* **15**, 5280 (1996).
9. W. G. Whitfield, C. Gonzalez, G. Maldonado-Codina, D. M. Glover, *ibid.* **9**, 2563 (1990).
10. T. Hunt, F. C. Luca, J. V. Ruderman, *J. Cell Biol.* **116**, 707 (1992).
11. S. Sigrist, H. Jakobs, R. Stratmann, C. F. Lehner, *EMBO J.* **14**, 4827 (1995).
12. N. Sethi, M. C. Monteagudo, D. Koshland, E. Hogan, D. J. Burke, *Mol. Cell. Biol.* **11**, 5592 (1991).
13. I. A. Dawson, S. Roth, S. Artavanis-Tsakonas, *Development* **117**, 359 (1993).
14. ———, *ibid.* **129**, 725 (1995).
15. W. Zachariae and K. Nasmyth, *Mol. Biol. Cell* **7**, 791 (1996).
16. All strains were derivatives of strain W303. *CLB2*, *PDS1*, and *ASE1* constructs were as described (*1*, *3*, *7*). Immunoprecipitations of ^{35}S-labeled Clb2 protein and DNA content analysis were performed as described (*7*). Protein immunoblot analysis of the total amount of Pds1, Ase1, and Cdc28 was done as described (*1*, *7*).
17. To generate a *GAL-CDC20* fusion, we engineered a Bgl II site at the AUG of *CDC20* and ligated it to an Eco RI to Bam HI fragment carrying the *GAL1-10* promoter. The fusion was integrated at the *URA3* locus.
18. R. Visintin, S. Prinz, A. Amon, unpublished observations.
19. W. R. Pearson and D. J. Lipman, *Proc. Natl. Acad. Sci. U.S.A.* **85**, 2444 (1988).
20. The probability score for Cdc20 and YGL003Cp being randomly related was 8×10^{-30}. The next lowest score was 3×10^{-6} for the ORF YRC72C, which also encodes a putative WD40-repeat protein.
21. S. F. Altschul, W. Gish, W. Miller, E. W. Myers, D. J. Lipman, *J. Mol. Biol.* **251**, 403 (1990).
22. A 1.8-kb fragment containing the *CDH1* gene was isolated from total genomic DNA by polymerase chain reaction. The *HIS3* gene was used to replace the *CDH1* ORF between the Nhe I and Blp I sites. The 1.8-kb fragment containing the *CDH1* gene was also used to generate a *GAL-CDH1* fusion that was integrated at the *URA3* locus.
23. Small G_1 phase daughter cells were elutriated as described (*28*). Nocodazole and hydroxyurea were added at concentrations of 15 μg/ml and 10 mg/ml, respectively.
24. M. D. Mendenhall, *Science* **259**, 216 (1993).
25. A. Amon, M. Tyers, B. Futcher, K. Nasmyth, *Cell* **74**, 993 (1993).
26. I. Fitch *et al.*, *Mol. Biol. Cell* **3**, 805 (1992).
27. D. Skowyra *et al.*, *Cell*, in press.
28. E. Schwob and K. Nasmyth, *Genes Dev.* **7**, 1160 (1993).
29. S. Irniger, S. Piatti, M. Michaelis, K. Nasmyth, *Cell* **87**, 269 (1995).

30. We thank O. Cohen-Fix, D. Koshland, and D. Pellman for antibodies and plasmids and V. Siegel, O. Cohen-Fix, D. Koshland, D. Pellman, S. Bell, D. Pellman, H. Madhani, T. Orr-Weaver, V. Mayer, A. Page, and M. Lane for helpful discussions and critical reading of the manuscript.

24 July 1997; accepted 19 September 1997

Forward and Backward Propagation of Dendritic Impulses and Their Synaptic Control in Mitral Cells

Wei R. Chen,* Jens Midtgaard, Gordon M. Shepherd

The site of impulse initiation is crucial for the integrative actions of mammalian central neurons, but this question is currently controversial. Some recent studies support classical evidence that the impulse always arises in the soma-axon hillock region, with back-propagation through excitable dendrites, whereas others indicate that the dendrites are sufficiently excitable to initiate impulses that propagate forward along the dendrite to the soma-axon hillock. This issue has been addressed in the olfactory mitral cell, in which excitatory synaptic input is restricted to the distal tuft of a single primary dendrite. In rat olfactory bulb slices, dual whole cell recordings were made at or near the soma and from distal sites on the primary dendrite. The results show that the impulse can be initiated in either the soma-axon hillock or in the distal primary dendrite, and that the initiation site is controlled physiologically by the excitatory synaptic inputs to the distal tuft and inhibitory synaptic inputs near the soma.

The mitral cell of the mammalian olfactory bulb gives rise to one apical dendrite (termed primary dendrite) and several lateral basal dendrites (termed secondary dendrites) (*1*). The primary dendrite extends 200 to 350 μm in the rat and enters a single glomerulus, where it ramifies in a distal tuft of branches that receive excitatory synaptic input from terminals of olfactory nerve (ON) (Fig. 1A). The secondary dendrites extend horizontally in the external plexiform layer (EPL), mediating recurrent and lateral synaptic inhibition through reciprocal dendrodendritic synapses with inhibitory granule cell interneurons (*2*).

As inferred by Ramon y Cajal in 1911 and established by later authors (*1*), the main function of the primary dendrite is clear: It links the synaptic response to olfactory input in the distal tuft to impulse output in the axon. This has served as one of the best examples proving that distal dendritic input is not limited to slow background modulation of soma output, but can mediate rapid information transmission (*3*). The location of excitatory synapses exclusively on the distal tuft thus furnishes an attractive model for investigating the role of dendrites in linking excitatory synaptic input to impulse output in a mammalian central neuron. In addition, the entirely separate location of granule cell inhibitory input to the soma and secondary dendrites provides a model for investigating the control of excitatory dendritic responses by synaptic inhibition.

Mitral cells were visualized in thick tissue slices of rat olfactory bulb under an infrared differential interference contrast (DIC) microscope (*4*–*6*). Primary dendrites were clearly visible and could be traced from the cell bodies all the way into individual glomeruli. Simultaneous whole cell recordings were made from the soma and at various distal sites on the primary dendrite near the glomerular tuft ($n = 24$ pairs from 22 slices). Dual dendritic recordings from proximal and distal sites (Fig. 1B; $n = 5$) gave results similar to those from soma and

W. R. Chen and G. M. Shepherd, Section of Neurobiology, Yale University School of Medicine, New Haven, CT 06510, USA.
J. Midtgaard, Department of Medical Physiology, University of Copenhagen, DK-2200 N, Copenhagen, Denmark.
*To whom correspondence should be addressed.